

Article

Effects of Alkali-Treatment and Feeding Route of Henequen Fiber on the Heat Deflection Temperature, Mechanical, and Impact Properties of Novel Henequen Fiber/Polyamide 6 Composites

Jeonghoon Kim and Donghwan Cho * 

Department of Polymer Science and Engineering, Kumoh National Institute of Technology, Gumi 39177, Korea; kjh40210@naver.com

* Correspondence: dcho@kumoh.ac.kr

Abstract: In the present study, novel natural fiber composites, consisting of untreated and alkali(NaOH)-treated chopped henequen fibers and polyamide 6 (PA6), were produced by the hopper feeding and side feeding of henequen fiber, upon the extrusion process, and then by an injection molding process, respectively. The effects of the alkali treatment and fiber feeding route on the heat deflection temperature, tensile, flexural, and Izod impact properties of henequen fiber/PA6 composites were investigated. The composite properties were increased by alkali treatment and further increased, considerably, by side feeding of the henequen fiber, being supported by inspecting the fiber length distribution and the fracture surface of resulting composites. It was clarified that the side feeding of chopped henequen fibers was preferable to increase the composite properties, compared to hopper feeding. This study may be worthy of processing and manipulating the properties of novel natural fiber composites, consisting of agave plant-derived henequen fiber and engineering plastic PA6.

Keywords: henequen fiber; polyamide 6; composite; alkali-treatment; feeding route; processing; properties



Citation: Kim, J.; Cho, D. Effects of Alkali-Treatment and Feeding Route of Henequen Fiber on the Heat Deflection Temperature, Mechanical, and Impact Properties of Novel Henequen Fiber/Polyamide 6 Composites. *J. Compos. Sci.* **2022**, *6*, 89. <https://doi.org/10.3390/jcs6030089>

Academic Editor: Francesco Tornabene

Received: 27 February 2022

Accepted: 11 March 2022

Published: 13 March 2022

Publisher's Note: MDPI stays neutral with regard to jurisdictional claims in published maps and institutional affiliations.



Copyright: © 2022 by the authors. Licensee MDPI, Basel, Switzerland. This article is an open access article distributed under the terms and conditions of the Creative Commons Attribution (CC BY) license (<https://creativecommons.org/licenses/by/4.0/>).

1. Introduction

Environmental pollution and regulations have been leading to the development of new materials, based on natural resources, over recent years. Accordingly, research and development on natural fiber-reinforced plastics, or polymer composites (NFRP), have increased in the last decades, to replace conventional glass fiber-reinforced plastics (GFRP) [1–4]. Plastics reinforced with plant-based or cellulose-based natural fibers, such as kenaf, flax, jute, hemp, henequen, sisal, etc., have attracted great attention as renewable materials, due to many advantages over GFRP, for many years. Industrial natural fibers, which can be easily used in NFRP, are inexpensive, light weight, biodegradable, easily processible with polymer resins, environmentally friendly, etc. However, plant-based natural fibers have some disadvantages, such as irregular fiber diameter and shape, limited processing temperature, poor fiber–polymer interfacial bonding, and possible composite strength reduction [2].

Henequen (*Agave fourcroydes*), which is a plant-based natural fiber and a native of the Yucatan Peninsula, Mexico, is a long, hard, and strong fiber, which can be industrially obtained from the 90–120 cm long leaves of agave plants, via retting and mechanical decortication processes. Henequen is quite similar with sisal (*Agave sisalana*) in appearance, but slightly lighter in color and marginally weaker. Henequen fiber has been extensively utilized to make twines, ropes, carpets, and cordages for a long period of time. In addition, it has often been used as reinforcement for making NFRP with thermoplastic or thermosetting polymers, due to its high specific stiffness and strength [5–7]. Henequen is composed of approximately 77% cellulose, 4–8% hemicellulose, 13% lignin, 2–6% pectin, and waxes [8,9].

The chemical compositions may be varied to a greater or lesser extent, depending on the henequen plant. Further, the fiber shape and diameter may be varied to some extent, according to the plantation location and the fiber position. Figure 1 displays photos of the henequen plant and the extracted henequen fiber.



Figure 1. Photos of henequen plant and the extracted henequen fiber.

Natural fibers, in general, exhibit low thermal resistance and limited processibility, upon exposure to processing temperatures higher than 200 °C, particularly in thermoplastics engineering, resulting in a decrease in composite properties. Polyamide 6 (PA6) is one of the widely used engineering plastics in industry, due to excellent mechanical properties, relatively low processing temperature, and good processibility. Accordingly, PA6 may be useful for making a composite material with environment-friendly natural fibers, if natural fiber would be successfully incorporated into the polymer matrix during composite fabrication. Nevertheless, NFRP with the polyamide matrix have rarely been studied, due to relatively high processing temperature, compared to general-purpose thermoplastics, such polypropylene and polyethylene, which can be processed at lower temperature during extrusion, injection, and compression molding processes [10,11].

Upon the extrusion process, the fiber feeding routes, such as hopper feeding and side feeding may significantly influence the composite properties. Jung and Cho [12] studied the effect of a carbon fiber feeding route during the extrusion process, on the electromagnetic, mechanical, and thermal properties of nickel-coated carbon fiber/polypropylene composites. They reported that the composites, with side-fed carbon fiber, exhibited the electromagnetic interference shielding effectiveness, tensile, flexural, and heat deflection temperature properties, higher than those with hopper-fed carbon fiber. It gave us research motivation, not only to fabricate novel henequen fiber/PA6 composites though an extrusion process with different feeding routes of henequen fiber, but also to enhance the properties of the resulting natural fiber composites.

The interfacial bonding between the natural fiber and polymer matrix is critically important in the interfacial, mechanical, and thermal properties of the resulting composites. In general, natural fibers of hydrophilic character have poor interfacial adhesion with a polymer matrix of hydrophobic character, particularly, lowering the mechanical properties of the resulting NFRP [1,13–15]. It has been found that the appropriate alkali treatment of natural fiber is effective to improve the properties of NFRP. Alkali treatment with sodium hydroxide (NaOH), under proper conditions, may play a role, not only in removing the hemicellulose component, waxes, and weak boundary layer existing on the natural fiber surface, but also in forming the chemical interaction between the fiber and the matrix and in roughening the fiber surface. As such, the fiber surface changes contribute to improving the fiber–matrix interfacial adhesion, leading to the increased composite properties [13,16].

Consequently, the objective of this work is, firstly, to produce novel henequen fiber-reinforced PA6 matrix composites, with 30 wt% fiber loading, via extrusion and injection molding processes, and secondly, to investigate the effects of alkali treatment and feeding route (hopper feeding, side feeding) of henequen fiber on the heat deflection temperature, tensile, flexural, and impact properties of henequen fiber/PA6 composites.

2. Materials and Methods

2.1. Materials

Henequen used in this work was kindly supplied from Centro de Investigación Científica de Yucatán, Mérida, Yucatan Peninsula, Mexico. Henequen fibers were extracted from the leaves of henequen plant by retting and mechanical decortication. The supplied henequen fiber bundles were 70–80 cm in length. The diameter of the single henequen fiber in the bundle was in the range of 150–250 μm . PA6 pellets (KN136, KOLON Plastics Co., Gimcheon-si, Korea) were used as matrix of the composite. NaOH powder was purchased from Dae Jeong Chemical Co., Seoul, Korea, and 6 wt% NaOH dissolved in distilled water, which was most effective to improve the interfacial bonding between the fiber and the matrix of natural fiber composites, as found in our earlier study [14], and was used throughout this work.

2.2. Surface Treatment of Henequen Fiber

The henequen fiber bundles were treated with 6 wt% NaOH solution for 1 h in a 5 L beaker using an ultrasonic bath (40 kHz, 400 W, Power Sonic 510, Hwashin Instrument Co., Ltd., Seoul, Korea). All the treated bundles were rinsed with flowing tap water for 15 min until pH 7 was obtained. The ‘as-received’ (untreated) henequen fiber bundles were also used for comparison. Both untreated and alkali-treated fiber bundles and PA6 pellets were sufficiently dried at 70 °C for 6 h in an air-circulating convection oven. The untreated and alkali-treated fiber bundles were chopped to be 4–6 mm long by using a chopping machine (DHS-28, Man Pyung Co., Seoul, Korea) prior to extrusion processing.

2.3. Processing of Henequen Fiber/PA6 Composites

Chopped henequen fibers and PA6 pellets were compounded by using a twin-screw extruder. The fiber loading was 30 wt%. Extrusion process was performed by using a modular intermeshing co-rotating-type twin-screw extruder (LG, BT-30-S2-421, Seoul, Korea) with the screw diameter of 30 mm and the L/D ratio of 42. The extruder barrel temperature was varied, depending on the barrel zone. Based on the result of preliminary work done to inspect the optimal processing conditions, the barrel temperature was set between 160–220 °C in the front zone, between 220–235 °C in the middle zone, and between 185–210 °C in the latter zone. The screw speed was 70 rpm. The main feeding rate was 10 kg/h and the side feeding rate was 40 kg/h. It was estimated that it normally took less than 2 min from the fiber feeding stage to the extruding stage at the die end. The henequen fiber/PA6 extrudate was directly and rapidly cooled down in a water bath right before being pelletized. Henequen fiber/PA6 pellets of roughly 3 mm long were obtained.

During extrusion process, chopped henequen fibers were regularly fed into the extruder by using a hopper (H) and a side feeder (S), respectively. In the case of the untreated henequen fiber, henequen fiber/PA6 composites produced through hopper feeding and side feeding of henequen fiber are referred to as ‘H-untreated’ and ‘S-untreated’ hereinafter, respectively. In the case of the alkali-treated henequen fiber, henequen fiber/PA6 composites produced through hopper feeding and side feeding are referred to as ‘H-treated’ and ‘S-treated’ hereinafter, respectively. Figure 2 illustrates twin-screw extrusion process for producing untreated and alkali-treated henequen fiber/PA6 pellets via hopper feeding and side feeding of untreated and alkali-treated henequen fibers.

After drying the pellets over 12 h in an air-circulating convection oven, injection molding process was carried out using an injection molding machine (Model PRO-WD 80, Dongshin Hydraulics Co., Changwon-si, Korea). The barrel temperatures were in the range of 210 to 225 °C, depending on the barrel zone. The injection-molded henequen fiber/PA6 composites with the fiber contents of 30 wt% were used as specimens for heat deflection temperature, tensile, flexural, and impact tests. Figure 3 illustrates injection molding process to fabricate untreated and alkali-treated henequen fiber/PA6 composites.

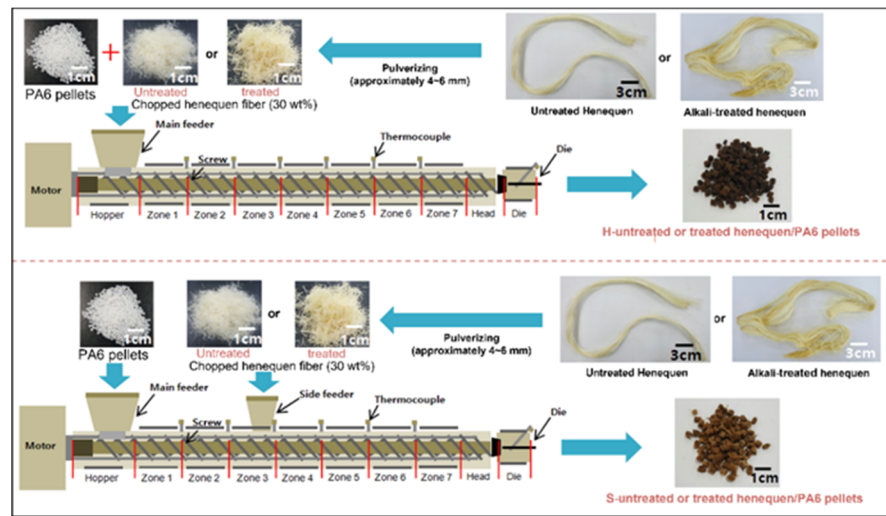


Figure 2. Illustration showing twin-screw extrusion process to prepare untreated and alkali-treated henequen fiber/PA6 pellets via hopper feeding and side feeding of henequen fiber, respectively.

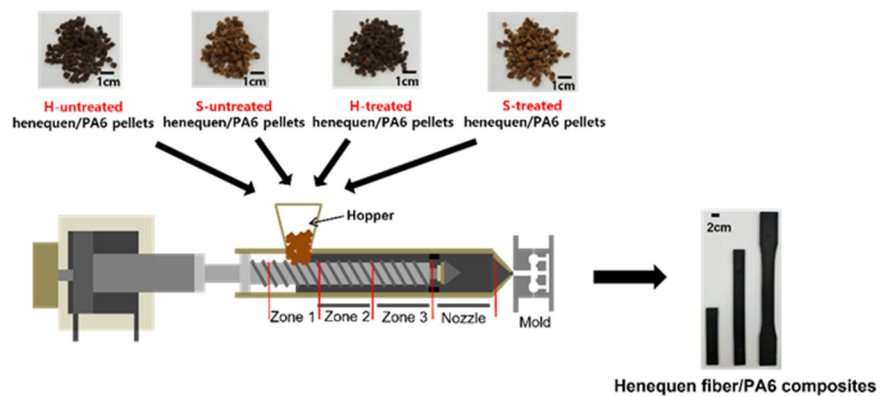


Figure 3. Illustration showing injection molding process to fabricate untreated and alkali-treated henequen fiber/PA6 composites.

2.4. Characterization

2.4.1. Fiber Surface Observation

The topography of untreated and alkali-treated henequen fiber surfaces was observed with the secondary electron image (SEI) mode using a scanning electron microscope (SEM, JSM-6380, JEOL, Fukuoka, Japan) after coating with platinum for 3 min. The electron voltage used was 15 kV.

2.4.2. Heat Deflection Temperature Measurement

Heat deflection temperature (HDT) of henequen fiber/PA6 composites was measured by means of HDT tester (Model 603, Tinius Olsen, Horsham, PA, USA) according to the ASTM-D648 standard. The specimen dimensions were 125 mm × 12.5 mm × 3 mm. The test was performed in a silicone oil bath heated at a heating rate of 120 °C/h after the specimen was soaked in the bath for 3–5 min. The heating rate for HDT measurement was 2 °C/min. Each test was carried out under the three-point bending load of 0.455 MPa. The HDT was determined at the temperature, where the specimen was deflected by 0.254 mm during the measurement. The average HDT of each composite was obtained from three specimens.

2.4.3. Tensile Test

Tensile tests were performed at ambient temperature using a universal testing machine (UTM, Shimadzu JP/AG-50kNX, Kyoto, Japan) according to the ASTM-D638M standard.

The dog-bone type specimens obtained from injection molding were used. The load cell used was 50 kN. The crosshead speed was 50 mm/min. The average values of tensile strength and modulus of each composite were obtained from ten specimens.

2.4.4. Flexural Test

Three-point flexural tests were performed at ambient temperature using a universal testing machine (UTM, Shimadzu JP/AG-50kNX, Kyoto, Japan) according to the ASTM-D790M standard. The dimensions of rectangular-shaped specimens were 125 mm × 12.5 mm × 3 mm. The span-to-depth ratio was 32. The load cell used was 50 kN. The crosshead speed was 5.1 mm/min. The average values of flexural strength and modulus of each composite were obtained from ten specimens.

2.4.5. Impact Test

Izod impact tests of the composites were carried out at ambient temperature according to the ASTM-D256 standard using a pendulum-type impact tester (Model 867, Tinius Olsen, Salfords, UK). The dimensions of each specimen were 65 mm × 12.5 mm × 3 mm. The V-shaped notch of each specimen was made by using a notch cutter according to the ASTM-D256 standard. Each test was performed with the pendulum impact speed of 3.46 m/s. The impact distance was 610 mm. The impact energy was 12.66 J. The average impact strength of each composite was obtained from ten specimens.

3. Results and Discussion

3.1. Temperature Effect on the Surface Topography and the Property of Henequen Fiber

Figure 4 displays SEM images ($\times 400$) observed with henequen fiber surfaces exposed at 235 °C for different heat-treatment times (0, 2, 5, and 10 min), in an air-circulating convection oven. The times (2, 5, and 10 min) at 235 °C were set to inspect how henequen fibers can be influenced by the highest temperature exposure (at 235 °C) in the barrel during the extrusion process. It was estimated that the exposure, or residence time, of henequen fiber, at the screw speed of 70 rpm in the heated barrel, was less than 2 min after each feeding of the chopped henequen fibers. As shown, there were some wax and weak boundary layers on the fiber surface and the striations and knobs were observed. With increasing exposure time, the henequen fiber was somewhat damaged, indicating fiber splitting behavior with some gaps along with the fiber direction. It seemed that the knobs were gradually removed.

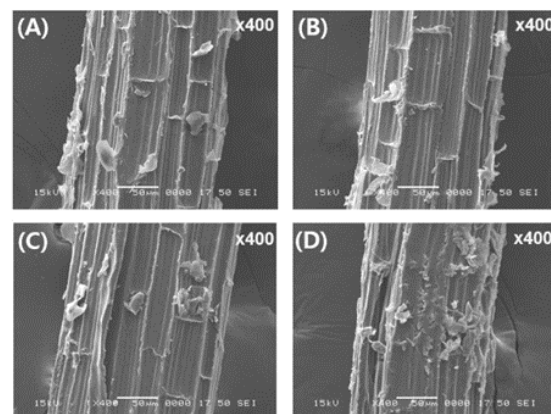


Figure 4. SEM images ($\times 400$) of the surfaces of henequen fibers heat treated for different times (A: 0 min, B: 2 min, C: 5 min, D: 10 min).

Figure 5 depicts the variations of the tensile modulus and strength for individual henequen fibers, measured as a function of heat-treatment time, described in Figure 4. Each value of the modulus and strength was averaged from 30 specimens, used for the

single fiber tensile test. The tensile modulus was decreased by 9%, whereas the tensile strength was decreased by 24%, upon 2 min exposure at 235 °C. It was expected that such a decrease in the tensile properties would be ascribed to the changes in the surface topography, such as fiber splitting, removal of the surface knobs, and loss of the fiber crystal structure by the heat-treatment. The fiber damages were also attributed to possible removal of hemi-cellulose and lignin components in the fiber [17].

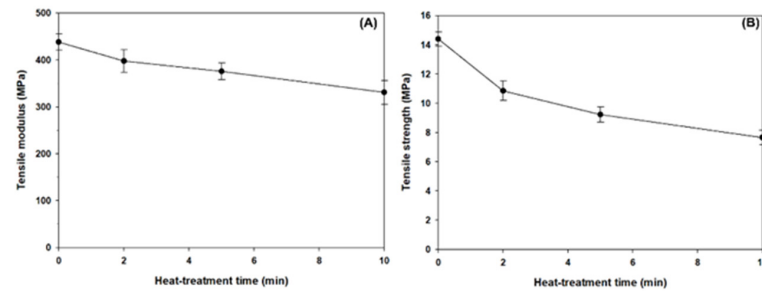


Figure 5. Variations of the tensile modulus (A) and strength (B) of henequen fibers exposed at 235 °C for different heat-treatment times, measured by a single fiber tensile test.

It seemed that the mechanical deterioration of the henequen fiber, due to the heat treatment for 2 min at 235 °C, where the exposure time was similar with the henequen fiber, was exposed to the highest temperature (235 °C) of the extruder barrel, which was less serious than expected. Accordingly, it was thought that the possible reduction in the mechanical properties of the henequen fiber, thermally exposed during extrusion, could be overcome by the fiber reinforcing effect, by alkali treatment, and further by appropriate fiber feeding.

3.2. Alkali treatment Effect on the Henequen Fiber Surface Topography

Figure 6 displays the SEM micrographs of untreated (A) and alkali-treated (B) henequen fiber surfaces, respectively. After the alkali treatment of the henequen fiber with 6 wt% NaOH, under the ultrasonic condition, the treated fiber showed more striations and fewer knobs on the fiber surfaces than the untreated one. It was, obviously, found that the surfaces were significantly roughened by the alkali treatment, indicating that some fibrillation occurred. As similarly found earlier [18], henequen fiber surfaces can be chemically changed by alkali treatment, resulting in the removal of the hemicellulose component therein. With the assistance of ultrasonication, the henequen fiber surfaces were also changed, showing some smoothness without knobs, along with the longitudinal direction and deep, roughened striations, along with the transverse direction. It revealed that the alkali treatment, exposed to a given ultrasonic frequency, resulted in the removal of waxes, surface impurities, and the weak boundary layer from the henequen fiber surfaces. It may be expected that, as such, the fiber surface change can importantly contribute to increasing the interfacial bonding between the henequen fiber and PA6 matrix, as studied with other composite systems, consisting of different natural fibers and polymer matrices [14,19–21].

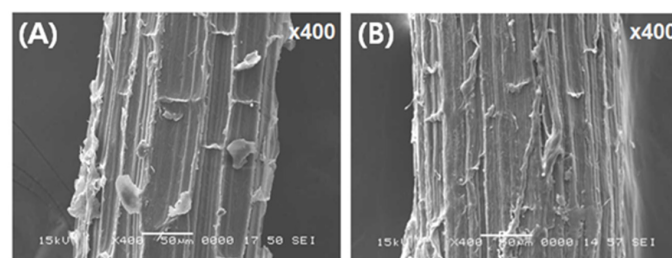


Figure 6. SEM images ($\times 400$) showing the henequen fiber surface topography (A: untreated, B: alkali treated).

3.3. Henequen Fiber Length Distribution

Figure 7 shows a histogram of the fiber length distribution, measured with the untreated henequen fiber/PA6 composites, produced through hopper feeding (H) and side feeding (S), respectively. The individual henequen fibers were obtained by dissolving the composite sample in a solvent and then separating the fibers from the PA6 matrix part. About 200 henequen fibers were used to count the fiber number, in the range of 50 to 650 μm in length. The average fiber length of 'H-untreated' composites was about 90 μm . The shortest fiber length was about 18 μm , and the longest length was about 397 μm . The average fiber length of 'S-untreated' composites was about 196 μm . The shortest fiber length was about 37 μm , and the longest length was about 633 μm . Further, in the case of 'H-untreated' composites, approximately 41% of the total number of the henequen fiber was about 50 μm . In the case of the 'S-untreated' composite, fibers of 50–100 μm in length were mostly found. As a result, the 'S-untreated' composite had a longer fiber length than the 'H-untreated' composite. This can be explained by the fact that the side feeding of chopped henequen fibers provided a shorter fiber path length than hopper feeding, experiencing less mechanical shear by the twin screws in the barrel during extrusion.

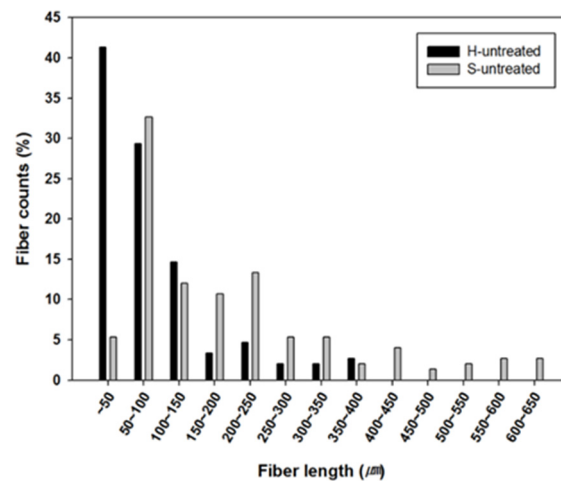


Figure 7. A histogram showing the henequen fiber length distribution measured with 'H-untreated' and 'S-untreated' henequen fiber/PA6 composites.

3.4. Heat Deflection Temperature

Figure 8 depicts the variation of HDT, measured with (H- and S-) untreated and (H- and S-) treated composites. The HDT values of the untreated composite were increased in comparison to the alkali-treated counterpart, and further increased by side feeding, compared to those by hopper feeding of the henequen fiber. This indicates that the HDT improvement of 'S-untreated' and 'S-treated' composites was ascribed to the reinforcing effect by the long henequen fiber distribution in the PA6 matrix. As mentioned, the HDT measurement was performed under the three-point bending load, with increasing temperature in a silicone oil bath. The HDT was sensitive to the thermal response of the composite specimen, consisting of chopped henequen fibers and PA6 matrix, present along with the through-thickness direction.

The through-thickness property of the composite can be significantly influenced by the interfacial bonding between the fiber and the matrix surrounding the individual fibers. The alkali-treated composite exhibited an HDT value higher than the untreated counterpart. This result indicates that the fiber feeding route, as well as the fiber surface treatment, were critically important, to increase the HDT of the henequen fiber/PA6 composite.

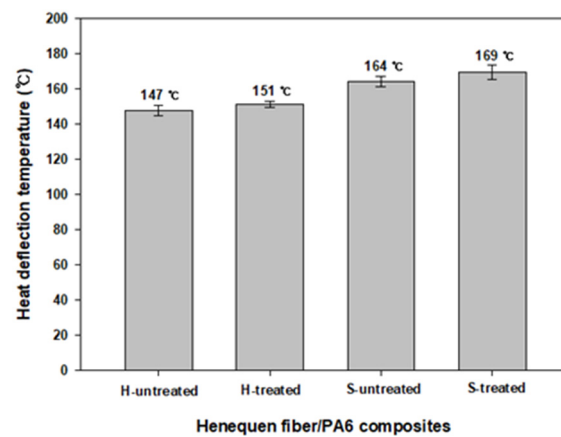


Figure 8. The HDT values measured with untreated or alkali-treated henequen fiber/PA6 composites produced via different fiber feeding routes.

3.5. Tensile Properties

Figure 9 compares the tensile modulus and strength of untreated and alkali-treated henequen fiber/PA6 composites, with different fiber feeding routes, respectively. The tensile modulus and strength exhibited a similar tendency, according to the feeding route and alkali treatment of the henequen fiber. It may be said that, compared to the side feeding case, the distribution of short fibers present in the composite, produced via hopper feeding, was mainly responsible for the lowered tensile modulus and strength of the composite. Furthermore, in the case of hopper feeding, henequen fibers were severely shortened and damaged because henequen fibers via hopper feeding can experience the longer residence time in the barrel than those via side feeding until extruded. Both the tensile modulus and strength were considerably increased, not only by the alkali treatment, but also by side feeding of the henequen fiber. As such the property enhancement was in good agreement with the HDT result, mentioned above.

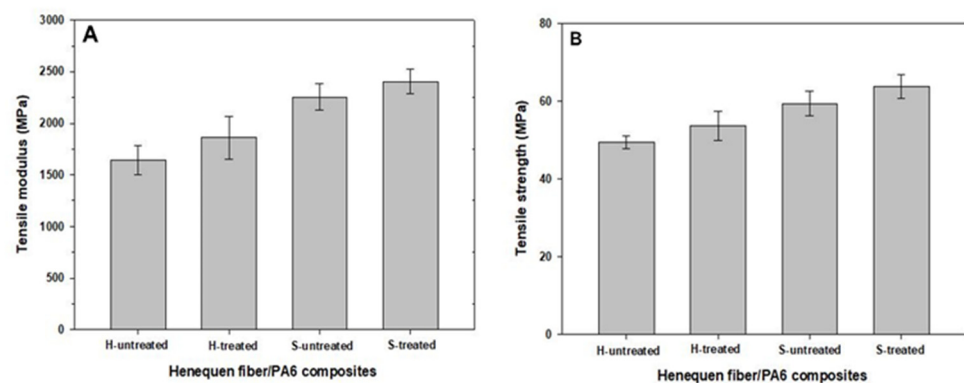


Figure 9. Tensile modulus (A) and strength (B) of untreated and alkali-treated henequen fiber/PA6 composites produced via different fiber feeding routes.

As similarly found in other natural fiber/polymer composites [13,22–25], the increase in tensile modulus was ascribed to the increased aspect ratio and the distribution of anisotropic fibers, resulting in the matrix stiffening, whereas the decrease in tensile strength was primarily influenced by microstructural defects, such as damage and void existing in the composite. The fiber damage and length degradation can result from the mechanical shear forces, by screw motion in the barrel, during the extrusion process. In addition, thermally damaged natural fiber may influence the composite property. It may be possible that henequen fibers were somewhat thermally damaged by relatively high processing temperatures, up to 235 °C, during the extrusion process, particularly in the case of hopper feeding, with the longer residence time of henequen with PA6 in the extruder barrel.

3.6. Flexural Properties

Figure 10 compares the flexural modulus and strength of the untreated and alkali-treated henequen fiber/PA6 composites, with different feeding routes, respectively. The flexural behavior was similar with the tensile behavior, according to the alkali treatment and feeding route of the henequen fiber, as seen in Figure 9. The explanation for the data variation in the tensile properties can also be given to the flexural properties.

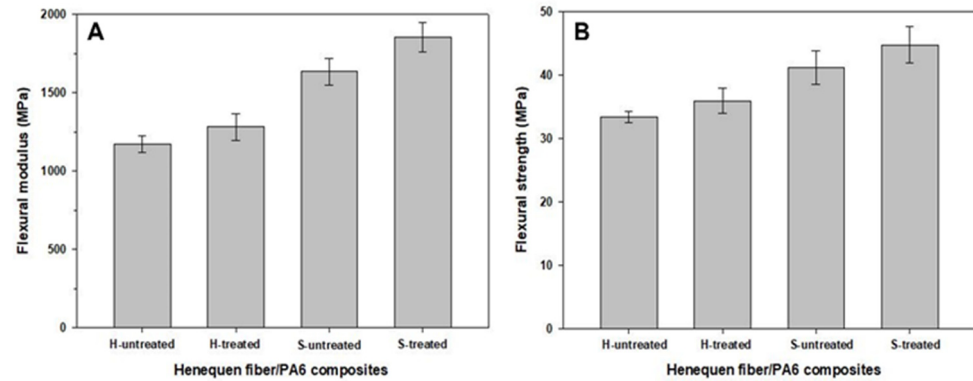


Figure 10. Flexural modulus (A) and strength (B) of untreated and alkali-treated henequen fiber/PA6 composites produced via different fiber feeding routes.

As a result, it can be said that both the alkali treatment and side feeding route played a positive role in enhancing the tensile and flexural properties of the henequen fiber/PA6 composite. It was noted that side feeding, rather than hopper feeding of the henequen fibers, was preferable to improve the modulus and strength under the processing conditions used in the present work.

3.7. Izod Impact Strength

Figure 11 shows the Izod impact strength of untreated and alkali-treated henequen fiber/PA6 composites, with different feeding routes. The impact strength of the untreated composite was increased by alkali treatment, and further enhanced by side feeding of the henequen fiber. This may be explained, not only by the lesser damage and defects of the henequen fibers in the composite produced via side feeding, but by the increased interfacial adhesion between the fiber and the matrix by the alkali treatment, which were responsible for the increased impact strength of the resulting composites.

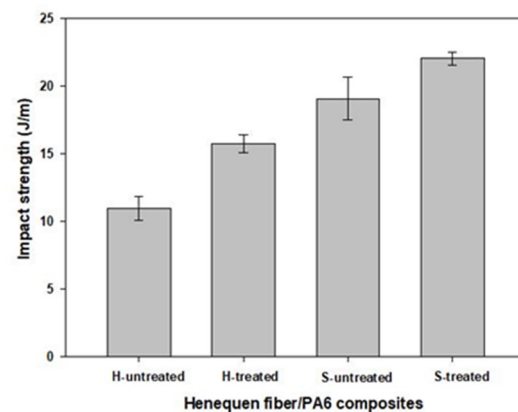


Figure 11. Izod impact strengths for untreated or alkali-treated henequen fiber/PA6 composites produced via different fiber feeding routes.

3.8. Fracture Surface Topography

Figure 12 displays the fracture surface topography observed with untreated and alkali-treated henequen fiber/PA6 composites, produced via different feeding routes. The ‘H-treated’ and ‘S-treated’ composites (c and d) exhibited tighter contacts at the interfaces between the henequen fiber and the PA6 matrix than ‘H-untreated’ and ‘S-untreated’ composites (a and b). The alkali-treated composite exhibited relatively flattened fracture surfaces. Further, fiber pull-out and fiber–matrix debonding phenomena were obviously found in the untreated composite. These fracture patterns indicate that the fiber–matrix interfacial adhesion of the alkali-treated composite was stronger than that of the untreated one, as similarly observed in other natural fiber composites [26–29]. In addition, ‘H-untreated’ and ‘H-treated’ composites (a and c) showed many shortly broken fibers upon composite fracture. It seemed that the henequen fiber, therein, was somewhat damaged during the extrusion process. It may be addressed that the result on the heat deflection temperature, tensile, flexural, and impact properties are quantitatively supported by the fracture surface topography.

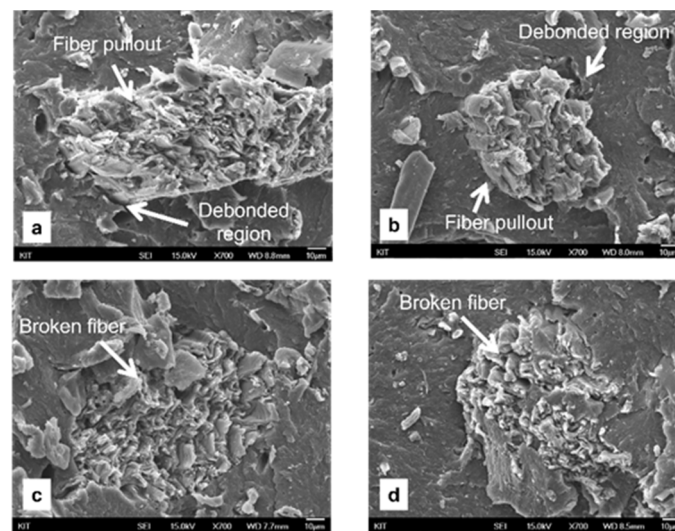


Figure 12. SEM images ($\times 700$) of the fracture surfaces of (a,b) untreated and (c,d) alkali-treated henequen fiber/PA6 composites produced via (a,c) hopper feeding and (b,d) side feeding.

4. Conclusions

Novel natural fiber composites, consisting of henequen fiber and PA6, were produced by an extrusion and injection molding technique. Upon the extrusion process, untreated and alkali-treated henequen fibers were regularly fed into the barrel, through the hopper and the side feeder, respectively. The effects of the alkali treatment and fiber feeding route, on the thermal, mechanical, and impact properties of henequen fiber/PA6 composites, were concluded as follows.

The heat deflection temperature, tensile, flexural, and Izod impact properties of NaOH-treated henequen fiber/PA6 composites, were higher than those of the untreated counterpart. The side feeding of chopped henequen fibers was preferable to enhance the fiber length distribution in the composite, compared to hopper feeding. As a result, the properties increased by alkali treatment were further enhanced, considerably, by the side feeding of the henequen fiber, upon the extrusion process. The fracture surface topography qualitatively supported the heat deflection temperature, tensile, flexural, and impact results. The present study demonstrated that uses of both the alkali treatment and side feeding route contributed importantly to improving the thermal, mechanical, and impact properties of a henequen fiber/PA6 composite.

Author Contributions: Conceptualization, writing—original draft preparation, writing—review and editing, supervision, formal analysis, funding D.C.; methodology, investigation, data curation, J.K. All authors have read and agreed to the published version of the manuscript.

Funding: This research was supported by Kumoh National Institute of Technology, Korea (2021).

Institutional Review Board Statement: Not applicable.

Informed Consent Statement: Not applicable.

Data Availability Statement: Not applicable.

Acknowledgments: The authors express their thanks to P. J. Herrera-Franco, at Centro de Investigación Científica de Yucatán, Mérida, Yucatan Peninsula, Mexico, for his kind supply of henequen fiber bundles, which were used in this work.

Conflicts of Interest: The authors declare no conflict of interest.

References

1. Cho, D.; Lee, S.G.; Park, W.H.; Han, S.O. Eco-friendly biocomposite materials using biofibers. *Polym. Sci. Technol.* **2002**, *46*, 460–476.
2. Joshi, S.V.; Drzal, L.T.; Mohanty, A.K.; Arora, S. Are natural fiber composites environmentally superior to glass fiber reinforced composites? *Compos. Part A* **2004**, *35*, 371–378. [[CrossRef](#)]
3. Fisher, R. Natural fibers and green composites. *Compos. Manufac.* **2006**, *3*, 20–23.
4. Cho, D.; Lee, H.S.; Han, S.O. Effect of fiber surface modification on the interfacial and mechanical properties of kenaf fiber-reinforced thermoplastic and thermosetting polymer composites. *Compos. Interf.* **2009**, *16*, 711–729. [[CrossRef](#)]
5. Canche-Escamilla, G.; Rodriguez-Laviada, J.; Cauich-Cupul, J.I.; Mendizabal, E.; Puig, J.E.; Herrera-Franco, P.J. Flexural, impact and compressive properties of a rigid-thermoplastic matrix/cellulose fiber reinforced composites. *Compos. Part A* **2002**, *33*, 539–549. [[CrossRef](#)]
6. Herrera-Franco, P.J.; Valadez-Gonzalez, A. Mechanical properties of continuous natural fibre reinforced polymer composites. *Compos. Part A* **2004**, *35*, 339–345. [[CrossRef](#)]
7. Pang, Y.; Cho, D.; Han, S.O.; Park, W.H. Interfacial shear strength and thermal properties of electron beam-treated henequen fiber reinforced unsaturated polyester composites. *Macromol. Res.* **2005**, *13*, 453–459. [[CrossRef](#)]
8. Cho, D.; Lee, H.S.; Han, S.O.; Drzal, L.T. Effects of e-beam treatment on the interfacial and mechanical properties of henequen/polypropylene biocomposites. *Adv. Compos. Mater.* **2007**, *16*, 315–334. [[CrossRef](#)]
9. Bismarck, A.; Mishra, S.; Lampke, T. Plant fibers as reinforcement for green composites. In *Natural Fibers, Biopolymers, and Biocomposites*; Mohanty, A.K., Misra, M., Drzal, L.T., Eds.; Taylor and Francis: Boca Raton, FL, USA, 2005; pp. 37–108.
10. Lee, S.; Shi, S.; Groom, L.H.; Xue, Y. Properties of unidirectional kenaf fiber-polyolefin laminates. *Polym. Compos.* **2010**, *31*, 1067–1074. [[CrossRef](#)]
11. Kim, J.; Cho, D. Effects of waste expanded polypropylene as recycled matrix on the flexural, impact, and heat deflection temperature properties of kenaf fiber/polypropylene composites. *Polymers* **2020**, *12*, 2578. [[CrossRef](#)]
12. Jung, S.; Cho, D. Effect of fiber feeding route upon extrusion process on the electromagnetic, mechanical, and thermal properties of nickel-coated carbon fiber/polypropylene composites. *Compos. Part B* **2020**, *187*, 107861. [[CrossRef](#)]
13. Cho, D.; Kim, H.J.; Drzal, L.T. Surface treatment and characterization of natural fiber: Effects on the properties of biocomposites. In *Polymer Composites Volume 3: Biocomposites*; Thomas, S., Joseph, K., Malhotra, S.K., Goda, K., Sreekala, M.S., Eds.; Wiley-VCH Verlag GmbH & Co.: Weinheim, Germany, 2013; pp. 133–177.
14. Lee, H.S.; Cho, D. Effect of natural fiber surface treatments on the interfacial and mechanical properties of henequen/polypropylene biocomposites. *Macromol. Res.* **2008**, *16*, 411–417. [[CrossRef](#)]
15. George, J.; Sreekala, M.S.; Thomas, S. A review on interface modification and characterization of natural fiber reinforced plastic composites. *Polym. Eng. Sci.* **2001**, *41*, 1471–1485. [[CrossRef](#)]
16. Herrera-Franco, P.J.; Valadez-González, A. Fiber-matrix adhesion in natural fiber composites. In *Natural Fibers, Biopolymers, and Biocomposites*; Mohanty, A.K., Misra, M., Drzal, L.T., Eds.; Taylor and Francis: Boca Raton, FL, USA, 2005; pp. 177–230.
17. Nada, A.M.A.; Kamel, S.; Sakhawy, M.E. Thermal behaviour and infrared spectroscopy of cellulose carbamates. *Polym. Degrad. Stab.* **2000**, *70*, 347–355. [[CrossRef](#)]
18. Cho, D.; Yoon, S.B.; Drzal, L.T. Cellulose-based natural fiber topography and the interfacial shear strength of henequen/unsaturated polyester composites: Influence of water and alkali treatments. *Compos. Interf.* **2009**, *16*, 769–779. [[CrossRef](#)]
19. Asumani, O.M.L.; Reid, R.G.; Paskaramoorthy, R. The effects of alkali-silane treatment on the tensile and flexural properties of short fibre non-woven kenaf reinforced polypropylene composites. *Compos. Part A* **2012**, *43*, 1431–1440. [[CrossRef](#)]
20. Aziz, S.H.; Ansell, M.P. The effect of alkalization and fibre alignment on the mechanical and thermal properties of kenaf and hemp bast fibre composites: Part 1—polyester resin matrix. *Compos. Sci. Technol.* **2004**, *64*, 1219–1230. [[CrossRef](#)]
21. Edeerozey, A.M.M.; Akil, H.M.; Azhar, A.B.; Ariffin, M.I.Z. Chemical modification of kenaf fibers. *Mater. Lett.* **2007**, *61*, 2023–2025. [[CrossRef](#)]

22. Lee, S.M.; Cho, D.; Park, W.H.; Lee, S.G.; Han, S.O.; Drzal, L.T. Novel silk/poly (butylene succinate) biocomposites: The effect of short fiber content on their mechanical and thermal properties. *Compos. Sci. Technol.* **2005**, *65*, 647–657. [[CrossRef](#)]
23. Huda, M.S.; Drzal, L.T.; Mohanty, A.K.; Misra, M. Effect of fiber surface-treatments on the properties of laminated biocomposites from poly (lactic acid) (PLA) and kenaf fibers. *Compos. Sci. Technol.* **2008**, *68*, 424–432. [[CrossRef](#)]
24. Ishiaku, U.S.; Yang, X.Y.; Leong, Y.W.; Hamada, H.; Semba, T.; Kitagawa, K. Effects of fiber content and alkali treatment on the mechanical and morphological properties of poly (lactic acid)/poly (carprolactone) blend jute fiber-filled biodegradable composites. *J. Biobased Mater. Bioener.* **2007**, *1*, 78–86. [[CrossRef](#)]
25. Qin, L.; Qiu, J.; Liu, M.; Ding, S.; Shao, L.; Lu, S.; Zhang, G.; Zhao, Y.; Fu, X. Mechanical and thermal properties of poly(lactic acid) composites with rice straw fiber modified by poly (butyl acrylate). *Chem. Eng. J.* **2011**, *166*, 772–778. [[CrossRef](#)]
26. Sreekala, M.S.; Kumaran, M.G.; Thomas, S. Oil palm fibers: Morphology, chemical composition, surface modification, and mechanical properties. *J. Appl. Polym. Sci.* **1997**, *66*, 821–835. [[CrossRef](#)]
27. Kalia, S.; Kaith, B.S.; Kaur, I. Pretreatments of natural fibers and their application as reinforcing material in polymer composites-a review. *Polym. Eng. Sci.* **2009**, *49*, 1253–1272. [[CrossRef](#)]
28. Gassan, J.; Bledzki, A.K. Possibilities for improving the mechanical properties of jute/epoxy composites by alkali treatment of fibres. *Compos. Sci. Technol.* **1999**, *59*, 1303–1309. [[CrossRef](#)]
29. Sreenivasan, S.; Bahama, I.P.; Krishnan, K.R.I. Influence of delignification and alkali treatment on the fine structure of coir fibres (*Cocos Nucifera*). *J. Mater. Sci.* **1996**, *31*, 721–726. [[CrossRef](#)]